MODELING THE EFFECT OF ELEVATED CO_2 AND CLIMATE CHANGE ON REFERENCE EVAPOTRANSPIRATION IN THE SEMI-ARID CENTRAL GREAT PLAINS

A. Islam, L. R. Ahuja, L. A. Garcia, L. Ma, A. S. Saseendran

ABSTRACT. *Changes in evapotranspiration demand due to global warming will have a profound impact on irrigation water demand and agricultural productivity. In this study, the effects of possible future anthropogenic climate change on reference evapotranspiration (ET_o) were evaluated using the Penman-Monteith equation. The combined effect of temperature and elevated CO_2 concentrations on ET_o was the major focus of this study. The ET_o under the General Circulation Model (GCM) projected climate change scenarios was estimated for a location in Colorado. Multi-model ensemble climate change scenarios were generated from 112 Bias Corrected and Spatially Disaggregated (BCSD) projections from the World Climate Research Program (WCRP) archive, which cover different levels of greenhouse gas emissions. Results showed a decrease in ET_o demand with increases in CO_2 levels, which greatly moderated the increase in ET_o due to increasing temperature. The effect of increases in CO_2 levels up to 450 ppm offset the effect of about 1°C rise in temperature. Simulation results with projected climate change scenarios, without considering the effects of CO_2 levels, showed an 8.3%, 14.7% and 21.0% increase in annual ET_o during the 2020s, 2050s, and 2080s, respectively, when simulation was carried out using an ensemble of the 112 projections. When the effect of elevated CO_2 levels was also considered in combination with projected changes in temperature, changes in annual ET_o demand varied from -1.5% to 5.5%, -10.4% to 6.7%, and -19.7% to 6.6% during the 2020s, 2050s, and 2080s, respectively, depending on the different climate change scenarios considered and the relationship or equation used for estimating the effect of elevated CO_2 on stomatal resistance term in the Penman-Monteith equation.*

Keywords. *Climate change, Evapotranspiration, Hybrid delta method, Multi-model ensemble scenario, Penman-Monteith equation, Stomatal resistance.*

Global climate change due to the enhanced greenhouse effect is likely to increase temperatures, alter precipitation patterns, and increase the frequency of extreme events. According to the Fourth Assessment Report of the Intergovernmental Panel on Climate Change (IPCC), the average global surface temperature is projected to increase by 1.1°C to 2.9°C for low greenhouse gas (GHG) emission scenarios and 2.4°C to 6.4°C for high GHG emission scenarios during 2090-2099 relative to 1980-1999 (IPCC, 2007). Consequently, significant changes in different components of the hydrological cycle are expected (Nash and Gleick, 1991). Evapotranspiration (ET) is the major component of the hydrological cycle and an important hydrological variable for irrigation water management and hydrological modeling. If a region becomes warmer, leading to increased evaporative demand, more irrigation water will be required to maintain crop yields. Uncertainty in the estimation of the potential evapotranspiration change signal is an important contributor to uncertainty in projections of global freshwater availability under conditions of climate change. Hence, improved understanding of changes in evapotranspiration is essential for improving confidence in such projections (Kingston et al., 2009).

Evapotranspiration represents the simultaneous processes of transfer of water to the atmosphere by transpiration and evaporation in a soil-plant system (Allen et al., 1998). The potential evapotranspiration demand for a crop depends mainly on air temperature, net solar radiation, relative humidity, and wind speed, as well as crop canopy characteristics (e.g., canopy height, leaf area index, and stomatal conductance). Martin et al. (1989) conducted sensitivity analyses using the Penman-Monteith (PM) equation and showed that evapotranspiration was highly sensitive to air temperature, solar radiation, humidity, and stomatal resistance. Irmak et al. (2006) conducted sensitivity analyses for the standardized daily form of the grass-reference ASCE-PM equation by increasing and decreasing an individual climate variable while keeping the other variables

Submitted for review in February 2012 as manuscript number SW 9630; approved for publication by the Soil & Water Division of ASABE in October 2012.

The authors are **Adlul Islam,** Senior Scientist, ICAR Research Complex for Eastern Region, Bihar Veterinary College, Patna, India; **Lajpat R. Ahuja, ASABE Member,** Research Leader, USDA-ARS Agricultural Systems Research Unit, Fort Collins, Colorado; **Luis A. Garcia, ASABE Member,** Professor, Department of Civil and Environmental Engineering, Colorado State University, Fort Collins, Colorado; **Liwang Ma,** Research Scientist, and **Anapalli S. Saseendran,** Research Scientist, USDA-ARS Agricultural Systems Research Unit, Fort Collins, Colorado. **Corresponding author:** Lajpat R. Ahuja, USDA-ARS Agricultural Systems Research Unit, 2150 Centre Avenue, Bldg. D, Suite 200, Fort Collins, CO 80526; phone: 970-492-7315; e-mail: Laj.Ahuja@ars.usda.gov.

and parameters constant. They found that reference evapotranspiration (ET_o) was most sensitive to vapor pressure deficit (VPD) and second most sensitive to wind speed. Elgaali et al. (2007) assessed the sensitivity of evapotranspiration to climatic variables in the Arkansas River basin in Colorado. Their study showed that evapotranspiration was more sensitive to changes in temperature and wind speed, while solar radiation and relative humidity had only slight impacts.

Increased atmospheric CO_2 levels have important physiological effects on crop plants, such as an increase in photosynthetic rate, leaf area, biomass, and yield, as well as reduction in stomatal conductance and transpiration per unit of leaf area (Allen, 1990; Kimball and Bernacchi, 2006; Kimball, 2007). Experimental results have indicated a decline in stomatal conductance in various plants with increase in atmospheric CO_2 levels, resulting in a reduction of transpiration (e.g., Morison and Gifford, 1983; Field et al., 1995; Saxe et al., 1998; Wand et al., 1999; Wullschleger et al., 2002). Total leaf area of some plant types may increase with increased atmospheric CO_2 levels (Saxe et al., 1998; Wand et al., 1999), leading to increased transpiration and potentially offsetting the effect of the reduction in stomatal conductance. Wand et al. (1999) reported 24% and 29% decrease in stomatal conductance and 15% and 25% increase in individual leaf area for C3 and C4 species, respectively, with doubling of CO_2 levels. Morgan et al. (2011) reported that elevated CO_2 can completely reverse the desiccating effects of moderate warming in a semi-arid grassland. In semi-arid grasslands, under a warmer and CO_2-enriched environment, the soil water content and productivity may be higher than previously expected. Ramirez and Finnerty (1996) found that the CO_2-induced effects on potential evapotranspiration (PET) were greater than those induced by temperature change for irrigated potato agriculture in the San Luis Valley of south central Colorado. They reported an 18.5% decrease in PET with a 3°C increase in temperature and doubling of CO_2 levels, and a 39% decrease in PET with a 3°C decrease in temperature combined with doubling of CO_2 levels. Martin et al. (1989) found that the effect of higher temperature on evapotranspiration could be either moderated or exacerbated by changes in the other climatic elements (radiation, humidity, wind) and in plant factors (leaf area index, stomatal resistance). They reported changes in evapotranspiration of about -20% to +40% depending on the ecosystem, climate, and plant type. McKenney and Rosenberg (1993) demonstrated that the sensitivity of potential evapotranspiration to changes in climate can vary by location, by time of year, and by differences in the climatic factors considered. Thus, for studying the effect of global warming on evapotranspiration, changes in temperature and other climatic variables and changes in plant growth and stomatal resistance caused by rising CO_2 levels need to be considered on a regional basis (Martin et al., 1989; Rosenberg et al., 1989; Allen et al., 1991). The ET_o is an important parameter and is used by scientists, extension workers, and growers as an agroclimatic indicator to quantify crop water needs and to schedule irrigation. Study on the effect of CO_2 and climate change on ET_o in semi-arid regions is needed, as there is a widely held perception that temperature changes will dramatically increase the evapotranspiration demand in future years.

There are several methods for estimation of reference evapotranspiration (ET_o), of varying complexity, with some requiring just one atmospheric variable (e.g., temperature) and others requiring several variables (e.g., temperature, relative humidity, solar radiation, wind speed). However, their performance varies under different climatic conditions. In the context of climate change, changes in atmospheric variables other than temperature may have a significant effect on the overall change in evapotranspiration demand. Thus, different ET_o estimation methods could produce different change signals (McKenney and Rosenberg, 1993; Kay and Davies, 2008; Kingston et al., 2009). While comparing potential evapotranspiration estimated using six commonly used potential evapotranspiration methods (Penman-Monteith, Hamon, Hargreaves, Priestley-Taylor, Blaney-Criddle, and Jensen-Haise) and using the global climate change signal of five different GCMs, Kingston et al. (2009) reported that the uncertainty between GCMs is lower than the uncertainty between methods within each individual GCM. The International Commission on Irrigation and Drainage (ICID) and the Food and Agricultural Organization (FAO) Expert Consultation Committee on Revisions of FAO methodologies for crop water requirements have recommended the FAO-56 Penman-Monteith (PM) method as the standard method for estimation of ET_o (Allen et al., 1998). The FAO-56 method explicitly incorporates both energy and biophysical parameters. This method is based on a hypothetical reference crop with an assumed crop height of 0.12 m, a fixed surface resistance of 70 s m^{-1}, and an albedo of 0.23 and can be used in a wide variety of climatic conditions (Allen et al., 1998) without any need for adjustments of parameters. This method is also preferable for climate change impact studies, as it includes the effects of chauges in more atmospheric variables (Kay and Davies, 2008; Kingston et al., 2009). Further, the effect of elevated CO_2 levels on evapotranspiration can be accounted for by modifying the canopy resistance term in the PM equation (Ficklin et al., 2009; Parajuli, 2010; Wu et al., 2011).

GCMs are the primary tool for simulating the response of the global climate system to iucreasing greenhouse gas concentrations, and they provide estimates of changes in climate variables on a coarser scale. Therefore, spatial downscaling to scales more representative of the local area of interest is required (Christensen and Lettenmaier, 2007). There are a number of GCMs developed by different organizations around the world that contributed to the Third Coupled Model Intercomparison Project (CMIP3; Meehl et al., 2007). The outputs of different GCMs vary considerably, and hence the selection of the best GCM also becomes an issue. In the recent years, there has been growing interest in the use of ensembles of multiple GCMs and emission scenarios in impact assessment studies to account for the uncertainty associated with individual GCM projections (Raff et al., 2009). Reifen and Toumi (2009) concluded that the mean of multi-model ensemble of all the available Fourth Assessment Report (AR4) models provided the most reasonable basis for obtaining the best projections of future climate change. In this study, 112 bias-corrected and spatially disaggregated (BCSD) projections from the World

Climate Research Program's (WCRP) CMIP3 climate projections archive (Maurer et al., 2007) were used to generate four different multi-model ensemble climate change scenarios using different combinations of GCM projections for assessing the impact of climate change on ET_o. The first scenario comprised an ensemble of all 112 available projections; the other three scenarios comprised of 36, 39, and 37 projections representing B1 (low), A1B (medium), and high (A2) emission paths, respectively.

The present study focuses on the effect of elevated CO_2 levels and climate change on evapotranspiration demand in the semi-arid Central Great Plains of the U.S. using four different multi-model ensemble climate change scenarios. The sensitivity of the reference evapotranspiration (ET_o) to changes in temperature and elevated CO_2 levels was first evaluated. Changes in ET_o under different climate change scenarios with or without the effects of elevated CO_2 levels were then assessed. Further, as stomatal resistance varies with plant species, effect of two different forms of CO_2 response functions were also compared.

Data and Methodology

Observed climate data for a site in Greeley, Colorado (40.45° N, 104.64° W) were used as the baseline dataset for studying climatic change impacts on evapotranspiration demand. Daily weather data (minimum and maximum temperature, wind speed, and solar radiation) for the period 1992-2010 were obtained from the Colorado Agricultural Meteorological Network (CoAgmet) website (http://ccc.atmos.colostate.edu/~coagmet/). These data were supplemented by data from a nearby National Climatic Data Center weather station at the University of Northern Colorado, Greeley, for the period 1950-1991. Daily gridded observed data (1/8° resolution) obtained from the WCRP's Coupled Model Intercomparison Project phase 3 (CMIP3) dataset (Maurer et al., 2007) were used to fill the gaps in the base data. In order to study the potential impact of the projected climate change, 112 bias-corrected and spatially disaggregated (BCSD) projections from the World Climate Research Program (WCRP) archive (Meehl et al., 2007) were used. The 112 BCSD climate projections are comprised of 16 different CMIP3 models (table 1) with different initial conditions (runs) simulating three different GHG emissions scenarios: B1 (low), A1B (medium), and A2 (high) (IPCC, 2007).

FAO-56 Penman-Monteith Equation

The Penman-Monteith form of the combination equation for estimation of reference evapotranspiration can be expressed as (Allen et al., 1998):

$$\lambda ET_o = \frac{\Delta(R_n - G) + \rho_a c_p \dfrac{(e_s - e_a)}{r_a}}{\Delta + \gamma\left(1 + \dfrac{r_s}{r_a}\right)} \quad (1)$$

where

ET_o = reference evapotranspiration (mm d^{-1})
λ = latent heat of vaporization (kPa $°C^{-1}$)
R_n = net radiation (MJ m^{-2} d^{-1})
G = soil heat flux density (MJ m^{-2} d^{-1})
ρ_a = density of air (kg m^{-3})
c_p = heat capacity of air (MJ kg^{-1} $°C^{-1}$)
γ = psychrometric constant (kPa $°C^{-1}$)
e_s = saturation vapor pressure (kPa)
e_a = actual vapor pressure (kPa)
$(e_s - e_a)$ = vapor pressure deficit (kPa)
Δ = slope of the vapor pressure-temperature curve (kPa $°C^{-1}$)
r_a = bulk boundary layer resistance of the canopy (s m^{-1})
r_s = bulk stomatal resistance of the canopy (s m^{-1}).

For a hypothetical reference crop with an assumed crop height of 0.12 m, a fixed surface resistance of 70 s m^{-1}, and an albedo of 0.23, the FAO-56 Penman-Monteith equation can be written as (Allen et al., 1998):

$$ET_o = \frac{0.408\Delta(R_n - G) + \gamma \dfrac{900}{T + 273} u_2 (e_s - e_a)}{\Delta + \gamma(1 + 0.34\, u_2)} \quad (2)$$

where T is the air temperature (°C) and u_2 is the wind speed at 2 m height (m s^{-1}).

Table 1. Different GCM scenarios considered in this study.

Model No.	Modeling Group and Country	WCRP CMIP3 Identification	A2 Runs	A1B Runs	B1 Runs
1	Bjerknes Centre for Climate Research, University of Bergen, Norway	BCCR-BCM2.0	1	1	1
2	Centre for Climate Modeling and Analysis (CCCma), Canada	CGCM31 (T47)	1-5	1-5	1-5
3	Centre National de Recherches Meteorologiques, Meteo-France, France	CNRM-CM3	1	1	1
4	CSIRO, Australia	CSIRO-Mk3	1	1	1
5	NOAA Geophysical Fluid Dynamics Laboratory, U.S.	GFDL-CM2.0	1	1	1
6	NOAA Geophysical Fluid Dynamics Laboratory, U.S.	GFDL-CM2.1	1	1	1
7	NASA Goddard Institute for Space Studies, U.S.	GISS-ER	1	1	1
8	Institute for Numerical Mathematics, Russian Academy of Science, Russia	INM-CM3.0	1	1	1
9	Institut Pierre Simon Laplace, France	IPSL-CM4	1	1	1
10	Center for Climate System Research (University of Tokyo), National Institute for Environmental Studies, and Frontier Research Center for Global Change, Japan	MIROC3.2 (medres)	1-3	1-3	1-3
11	Meteorological Institute of the University of Bonn (Germany), Meteorological Research Institute of KMA, Korea	ECHO-G	1-3	1-3	1-3
12	Max Planck Institute for Meteorology, Germany	ECHAM5/MPI-OM	1-3	1-3	1-3
13	Meteorological Research Institute, Japan	MRI-CGCM2.3.2	1-5	1-5	1-5
14	National Center for Atmospheric Research, U.S.	CCSM3	1-4	1-3, 5-7	1-7
15	National Center for Atmospheric Research, U.S.	PCM	1-4	1-4	2-3
16	Hadley Centre for Climate Prediction and Research, Met Office, U.K.	UKMO-HADCM3	1	1	1
		Total:	36	39	37

As the stomatal conductance varies with CO_2 levels, this effect can be incorporated into equation 3 by modifying the stomatal resistance value for elevated CO_2 levels. To account for the CO_2 effect on ET_o, equation 2 can be rewritten as:

$$ET_o = \frac{0.408\Delta(R_n - G) + \gamma \frac{900}{T+273} u_2 (e_s - e_a)}{\Delta + \gamma\left(1 + \frac{0.34^* u_2}{CO_2\text{-factor}}\right)} \quad (3)$$

where "CO_2-factor" is the factor to account for the effect of elevated CO_2 levels and is computed as the ratio of stomatal conductances at a given CO_2 level and at the baseline atmospheric CO_2 concentration (330 ppm).

The stomatal conductance at different CO_2 levels can be calculated using different relationships (Allen, 1990; Stockle et al., 1992). For simulating the effect of CO_2 levels on evapotranspiration Stockle et al. (1992) developed the following linear relationship for stomatal conductance as a function of CO_2 levels, based on 80 data sets comparing leaf conductance at 330 ppm and at 660 ppm of CO_2 concentration for a wide range of species including C3 and C4 crops:

$$g_{CO_2} = g\left[1.4 - 0.4\frac{CO_2}{330}\right] \quad (4)$$

where g_{CO2} is the modified conductance due to elevated CO_2 levels, g is the conductance without elevated CO_2 levels, and 330 represents the baseline atmospheric CO_2 concentration (ppm). Equation 4 is based on experimental observations of a 40% linear decrease in stomatal conductance between 330 and 660 ppm CO_2 concentrations (Morison and Gifford, 1983) and has been used in several impact assessment studies (Easterling et al., 1992; Ficklin et al., 2009; Parajuli, 2010; Wu et al., 2011).

Allen (1990) reported stomatal conductance responses of soybean (C3 crop), maize or sweet corn (C4 crop), and sweetgum (C3 woody species) for CO_2 levels over the range of 340 to 1000 µmol mol^{-1} and predicted a reduction in stomatal conductance of 41%, 47%, and 39% for soybean, sweet corn, and sweetgum, respectively, at a CO_2 concentration of 660 µmol mol^{-1} with respect to 330 µmol mol^{-1}. As the FAO-56 Penman-Monteith equation is based on a hypothetical crop of 0.12 m height, generally accepted as a grass reference crop similar to perennial ryegrass (C3 type grass), in this study the CO_2 response function for soybean (C3 crop) was selected, and the following relationship (Allen, 1990) is used:

$$g = 0.0485 - 7.00\times10^{-5}(CO_2) + 3.40\times10^{-8}(CO_2)^2 \quad (5)$$

Equation 5 is valid for 340 to 1000 ppm CO_2 concentrations and covers most of the projected ranges of CO_2 increase from 600 (B1 emission path) to 1250 ppm (A2) by the year 2100 (IPCC, 2007). Extrapolation of equation 4, which is valid in the range of 330 to 660 ppm, beyond 660 ppm will result in greater decrease in stomatal conductance (fig. 1) and lower estimation of ET_o (large decrease in ET_o). In this study, CO_2 levels up to 930 ppm were considered, and equations 4 and 5 were used to compare the effects of inclusion of different CO_2 response functions within the PM equation for estimating ET_o. Considering that equations 4 and 5 are valid for the stomatal conductance of 0.12 m tall C3 species of grass with a canopy resistance of 70 s m^{-1}, the CO_2-factor in equation 3 was computed and the daily ET_o was estimated using the procedure described in the FAO-56 guidelines (Allen et al., 1998).

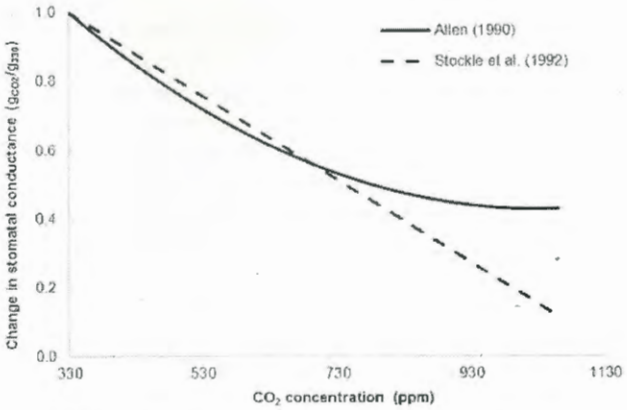

Figure 1. Effect of elevated CO_2 on stomatal conductance.

For estimating actual vapor pressure from temperature data (in the absence of relative humidity data), dew point temperature may be assumed to be near to the minimum temperature (i.e., $T_{dew} = T_{min}$) (Allen et al., 1998). However, in this study, the following empirical relationship, which has been developed using daily observed minimum and maximum temperature data at several locations in the northern U.S. Great Plains, i.e., Akron (Colo.), Gettysburg (S.D.), Gordon (Neb.), Hays (Kans.), Mead (Neb.), and North Platte (Neb.), was used to estimate the dew point temperature (Hubbard et al., 2003):

$$T_{dew} = -0.0360T_{max} + 0.9679T_{min} + 0.0072(T_{max} - T_{min}) + 1.0119 \quad (6)$$

Evaluation of ET_o Sensitivity to Temperature and CO_2 Changes

The combined effect of temperature and elevated CO_2 levels was studied by varying the temperature from 1°C to 5°C and the CO_2 level from 450 to 900 ppm. This range of temperature increases corresponds to the prediction of most of the GCMs for the study area. Different climate models project that Colorado will be 1.4°C warmer (1.5°C to 3.5°C) by 2025 relative to the 1950-1999 baseline and 2.2°C warmer (2.5°C to 5.5°C) by 2050 (Ray et al., 2008). As per the IPCC report (IPCC, 2007), CO_2 levels may reach 600, 850, and 1250 ppm by 2100 under the B1 (low), A1B (medium), and A2 (high) emission scenarios, respectively. For the sensitivity analysis, five different CO_2 levels (i.e., 450, 600, 660, 750, and 900 ppm) were considered.

Climate Change Scenario Generation

The most commonly used method for climate change scenario generation is to apply GCM scales projections in the form of change factors (CF), i.e., the "delta change" or

"perturbation" method (Hay et al., 2000; Ragab and Prudhomme, 2002). In this method, the differences between (or the ratio of) control and future climate simulations are applied to historical observations by simply adding (or multiplying) the change factor to daily observed data. This method does not account for variability or change in time series behavior in the future. Hamlet et al. (2010) reported a downscaling technique called the hybrid-delta (HD) method, which uses BCSD monthly time series of temperature and precipitation data downscaled to fine-scale grids (1/8° resolution). For climate change scenario generation using the HD method, BCSD monthly data for the selected location (grid point) were disaggregated into individual calendar months, and the cumulative distribution function (CDF) for each of the month was developed for historical (1950-1999) and future time periods (2020s, 2050s, and 2080s), which are referred to as historical and future CDFs, respectively. Similarly, the CDF for each month was developed from the observed time series data (1950-1999), referred to as observed CDF. Then for each month, quantile mapping (Wood et al., 2002) was done to re-map the observations onto the bias-corrected GCM data to produce a set of transformed observations reflecting the future scenario. In other words, for a given observed temperature for a given month, non-exceedance probability was first computed from the observed CDF. Then, corresponding to this non-exceedance probability level, the historical and future temperature values from their respective CDFs were computed. The difference between the future and historical temperature values was the resultant change factor. Thus, in this method, 50 factors were generated for each month (one for each year for the period 1950-1999) as compared to one factor for each month in the case of the delta change method. This method allowed for consideration of interannual variability for each month. For creating an ensemble of *n* projections, *n* number of BCSD projections were considered while constructing a historical and future CDFs. Using the above methodology, the following multi-model ensemble climate change scenarios were generated in this study:

S1: Ensemble of all 112 available projections (table 1).

S2: Ensemble of 37 projections representing the lower (B1) emission path.

S3: Ensemble of 39 projections representing the middle (A1B) emission path.

S4: Ensemble of 36 projections representing the higher (A2) emission path.

For simulating the impact of projected climate change on ET_o, the projected changes in temperature corresponding to the above four scenarios were superimposed on the observed baseline data series for the period 1950-1999. Simulation runs were made using the above four ensemble scenarios with and without elevated CO_2 levels for three different periods: 2020s (representing 2010-2039), 2050s (2040-2069), and 2080s (2070-2099). For the B1, A1B, and A2 emission paths, CO_2 levels of 600, 850, and 1250 ppm by 2100 were considered (IPCC, 2007). For the ensemble of the 112 projections, the average CO_2 level for the three emission paths was considered.

Results and Discussion

Effect of Temperature and Elevated CO_2 on ET_o

The combined effects of changes in temperature and CO_2 levels on reference evapotranspiration, estimated using equation 5 within the PM equation (eq. 3), indicated an increase in the annual ET_o demand from 1300 mm under the baseline scenario (no change in temperature and 330 ppm CO_2 concentration) to 1692 mm with a 5°C increase in temperature and 330 ppm CO_2 concentration (fig. 2). Thus, there is about a 30% increase in annual ET_o with a 5°C increase in temperature and a CO_2 concentration of 330 ppm. Every 1°C rise in temperature resulted in about a 6% increase in annual ET_o with CO_2 levels less than 450 ppm, but this value decreased to about a 5% with CO_2 levels of 900 ppm (fig. 2). If the temperature remains constant, then there is a decrease in ET_o with increase in CO_2 levels. With doubling of the CO_2 concentration (660 ppm) and no change in temperature, annual ET_o demand was estimated as 1147 mm, indicating about a 12% decrease in annual ET_o as compared to the baseline value. An increase of 5°C in temperature coupled with doubling of CO_2 levels resulted in a 15.5% increase in annual ET_o. Simulating the combined effect of temperature and elevated CO_2 levels also showed that the effect of increase in CO_2 levels up to 450 ppm was offset by about a 1°C rise in temperature, whereas the effect of doubling the CO_2 concentrations (660 ppm) was offset by about a 2°C rise in temperature. Monthly analysis showed an increase in ET_o in most of the months at a 2°C temperature rise and CO_2 concentrations of 450 ppm (table 2) with a maximum increase of 0.4 mm d^{-1} in mean monthly ET_o during May. However, the relative changes (%) with respect to the baseline scenarios showed maximum and minimum increase in ET_o during December and July, respectively. With a 4°C temperature rise, there was an increase in monthly ET_o for all months with a CO_2 level up to 900 ppm when equation 5 was used for estimation of the CO_2 effect on stomatal conductance. However, equation 4 resulted in a decrease in mean monthly ET_o at a CO_2 concentration of 900 ppm and temperature rise of 4°C.

A comparison of the different relationships (eqs. 4 and 5) used for estimating the CO_2 effects on ET_o (table 2) showed that both the equations produced similar results for CO_2 level

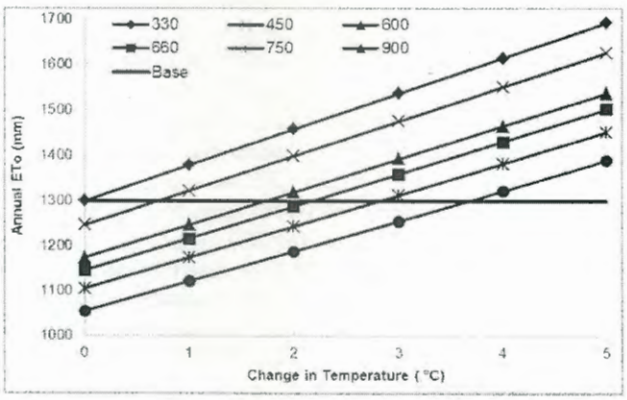

Figure 2. Effect of changes in temperature and CO_2 concentration on reference evapotranspiration.

Table 2. Effect of temperature and CO_2 changes on the reference evapotranspiration.

Temperature Change	Month	Reference Evapotranspiration (mm d^{-1})[a]								
			450 ppm		660 ppm		750 ppm		900 ppm	
		Base	A	S	A	S	A	S	A	S
2°C	January	1.5	1.8	1.8	1.5	1.4	1.4	1.3	1.3	0.9
	February	2.0	2.2	2.2	1.9	1.8	1.8	1.7	1.7	1.2
	March	2.7	3.0	3.0	2.7	2.6	2.5	2.3	2.4	1.8
	April	3.8	4.1	4.1	3.7	3.6	3.5	3.3	3.4	2.6
	May	4.8	5.2	5.2	4.8	4.6	4.6	4.3	4.4	3.6
	June	5.9	6.2	6.2	5.8	5.7	5.7	5.4	5.5	4.6
	July	6.0	6.3	6.3	6.0	5.9	5.9	5.7	5.7	5.0
	August	5.3	5.6	5.6	5.3	5.2	5.2	5.0	5.0	4.4
	September	4.2	4.5	4.5	4.2	4.1	4.1	3.9	3.9	3.3
	October	3.1	3.3	3.3	3.0	2.9	2.9	2.7	2.8	2.2
	November	1.9	2.1	2.1	1.9	1.8	1.8	1.6	1.7	1.2
	December	1.4	1.7	1.7	1.4	1.4	1.4	1.2	1.3	0.9
4°C	January	1.5	2.1	2.1	1.8	1.7	1.7	1.6	1.6	1.1
	February	2.0	2.6	2.6	2.3	2.2	2.2	2.0	2.0	1.5
	March	2.7	3.5	3.5	3.1	3.0	2.9	2.7	2.8	2.1
	April	3.8	4.6	4.6	4.2	4.0	4.0	3.7	3.8	3.0
	May	4.8	5.7	5.7	5.2	5.1	5.1	4.8	4.9	4.0
	June	5.9	6.6	6.6	6.3	6.1	6.1	5.8	5.9	5.0
	July	6.0	6.7	6.7	6.4	6.3	6.3	6.1	6.1	5.4
	August	5.3	6.0	6.0	5.7	5.6	5.6	5.4	5.4	4.7
	September	4.2	4.9	4.9	4.6	4.5	4.5	4.3	4.3	3.6
	October	3.1	3.7	3.7	3.4	3.3	3.3	3.1	3.1	2.5
	November	1.9	2.5	2.5	2.2	2.1	2.1	1.9	2.0	1.5
	December	1.4	2.0	2.0	1.7	1.7	1.6	1.5	1.5	1.1

[a] Base = ET_o with respect to base value (no change in temperature and CO_2), A = Allen (1990) equation 5 is used for CO_2 effects, and S = Stockle et al. (1992) equation 4 is used for CO_2 effects.

of 450 ppm. For CO_2 levels greater than 660 ppm, equation 4 resulted in lower ET_o estimates (greater decrease in ET_o) as compared to equation 5. This is due to the linear extrapolation of equation 4 beyond 660 ppm, as it estimated a greater decrease in stomatal conductance as compared to equation 5 with CO_2 levels above 660 ppm, as shown in figure 1.

Effect of Climate Change Scenario on ET_o

Climate change scenarios generated using the hybrid delta ensemble method showed large interannual variability in temperature increase during different months (fig. 3). However, average increase in temperature during different months varied in the range of 0.97°C (Nov.) to 1.75°C (Aug.), and 1.00°C (Apr.) to 1.73°C (Aug.) under the low (S2) and high (S4) emission scenarios, respectively, during the 2020s. During the 2080s, average increase in temperature during different months varied in the range of 2.18°C (Mar.) to 3.26°C (Sept.), and 3.37°C (Mar.) to 5.43°C (Sept.) under the low (S2) and high (S4) emission scenarios, respectively.

Simulation results with projected changes in temperature, without considering the effect of elevated CO_2 concentrations, showed an increase in ET_o for all the scenarios (fig. 4). The comparison of ET_o estimated using different scenarios showed that during the 2020s, all the scenarios (without considering the effect of CO_2 levels) produced similar results, with an average annual ET_o demand ranging from 1404 (S4) to 1412 mm (S3) compared to the baseline annual ET_o demand of 1300 mm. During the 2050s and 2080s, the estimated annual ET_o demand ranged from 1462 (S2) to 1511 mm (S3) and from 1508 (S2) to 1633 mm (S4), respectively. The increase in annual ET_o demand ranged from 7.9% to 8.6%, from 12.5% to 16.2%, and from 16.0% to 25.6% during the 2020s, 2050s, and 2080s, respectively. These changes depended on the climate change scenario being considered. Under the high emission scenario (A2), there was a 7.9%, 15.5%, and 25.6% increase in ET_o during the 2020s, 2050s, and 2080s, respectively (table 3). Under the low emission scenario (B1), there was an 8.4%, 12.5%, and 16.0% increase in annual evapotranspiration demand during the 2020s, 2050s, and 2080s, respectively. Simulation with the ensemble of all 112 projections (which includes projections from all three emission scenarios), resulted in 8.3%, 14.7%, and 21.0% increases in annual ET_o during the 2020s, 2050s, and 2080s, respectively.

Simulation results showed an increase in annual ET_o (as compared to the baseline ET_o) during the 2020s for all the scenarios, even when the effect of elevated CO_2 concentrations was considered along with projected changes in temperature, except for the high emission scenario (S4) (fig. 4). In the case of the high emission scenario (S4), changes in ET_o during the 2020s were almost negligible, and estimated ET_o resulted in a similar cumulative distribution curve as that of the baseline when the effect of increased CO_2 concentrations was considered along with the changes in temperature. During the 2080s, there was a decrease in annual ET_o for all scenarios except the low emission scenario (S2) when equation 4 was used with the PM equation. When equation 4 was used, under the high emission scenario (S4) the changes in annual ET_o ranged from -19.7% (2080s) to 0.6% (2020s), whereas for the low emission scenario (S2) it ranged from 5.5% (2020s) to 6.6% (2080s). However, when equation 5 was used for estimating the CO_2 effect on stomatal conductance, the estimated change in annual ET_o varied in the range of -2.5% (2050s) to 2.7% (2080s), and 5.5% (2020s) to 7.2% (2080s) under the high (S4) and low (S2) emission scenarios, respectively. In general, application of equations 4 and 5 for estimating the CO_2 effect on stomatal conductance produced comparable results with

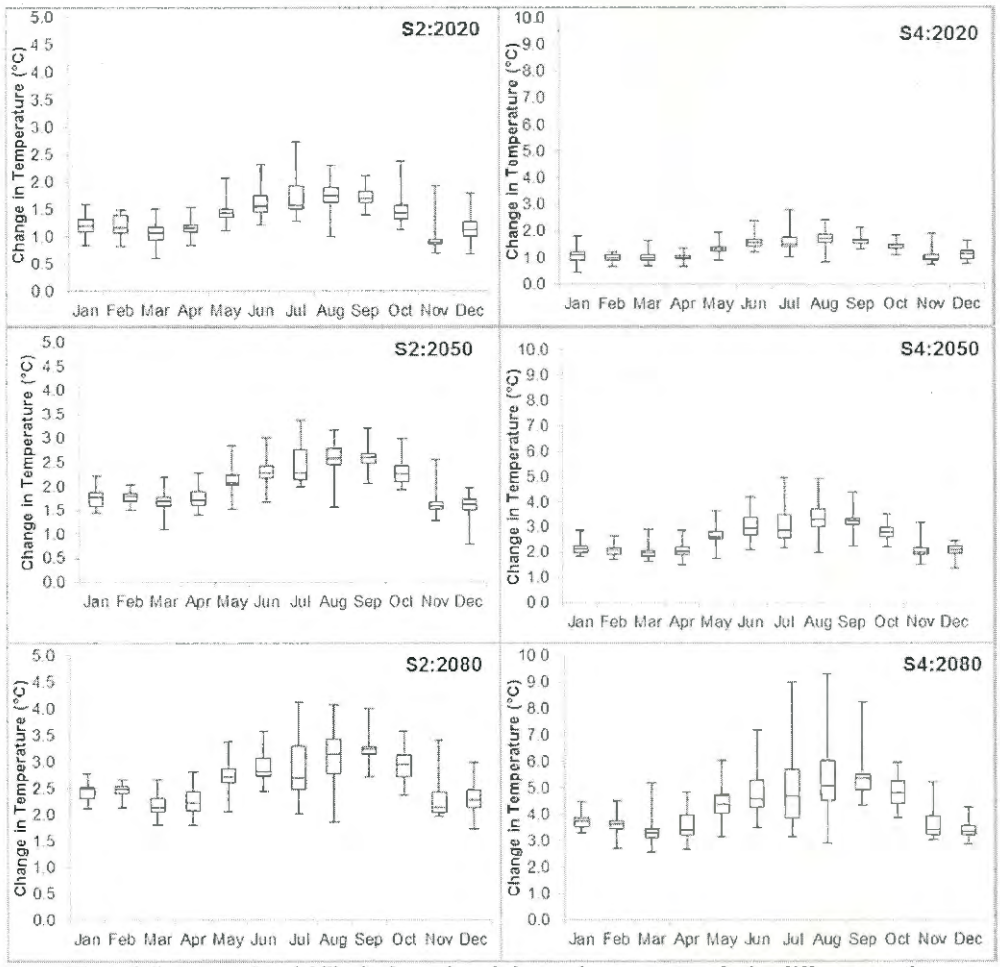

Figure 3. Interannual variability in the projected changes in temperature during different months.

projected changes in temperature at lower CO_2 levels; however, at higher CO_2 levels, particularly during the 2080s under the high emission scenario (S4), there was a large variation in ET_o. These results suggest the need for interpreting the results with caution when using different relationships for estimating the effect of CO_2 levels on stomatal conductance, which affects ET_o. The effect of rising temperature was almost mitigated by increasing CO_2 levels, with ET_o changes remaining below 10% in most of the cases.

Monthly analysis (table 3) showed variations in the changes in ET_o during different months. The magnitude of changes, as compared to the baseline, in ET_o during different months varied in the range of 0.2 to 0.4 mm d^{-1} during the 2020s for all scenarios under the projected changes in temperature. During the 2080s, the changes in ET_o during different months varied in the range of 0.5 to 1.0 mm d^{-1}, 0.4 to 0.8 mm d^{-1}, 0.6 to 1.0 mm d^{-1}, and 0.7 to 1.2 mm d^{-1} under the S1, S2, S3, and S4 scenarios, respectively. The relative changes in ET_o demand (with respect to the baseline scenario of no change in temperature and CO_2 concentration of 330 ppm) during different months varied in the range of 5.9% to 13.5%, 9.9% to 24.9%, and 13.4% to 38.0% during the 2020s, 2050s, and 2080s, respectively, with projected changes in temperature under the S1 scenario (ensemble of all 112 projections). It should be noted that the magnitude of change in ET_o was maximum during May and minimum during December-January in most of the cases. But while comparing relative changes (%) with respect to the baseline scenario, July recorded the minimum increase in ET_o and January-December recorded the maximum increase in ET_o demand with the projected changes in temperature for all the scenarios. With projected changes in temperature under the high emission scenario (S4), a maximum ET_o increase of 26% (Dec.-Jan.) and 45% (Dec.-Jan.) was estimated during the 2050s and 2080s, respectively. When the effect of CO_2 level was considered by using equations 4 and 5, both equations produced similar monthly ET_o values during the 2020s. However, during the 2080s under the high emission scenario (S4), changes in ET_o during different months varied in the range of -33.7% (Dec.) to -10.0% (Aug.) when equation 4 was used. Equation 5 resulted in -4.5% to 7.2% change in ET_o during the same period for the high emission scenario (S4).

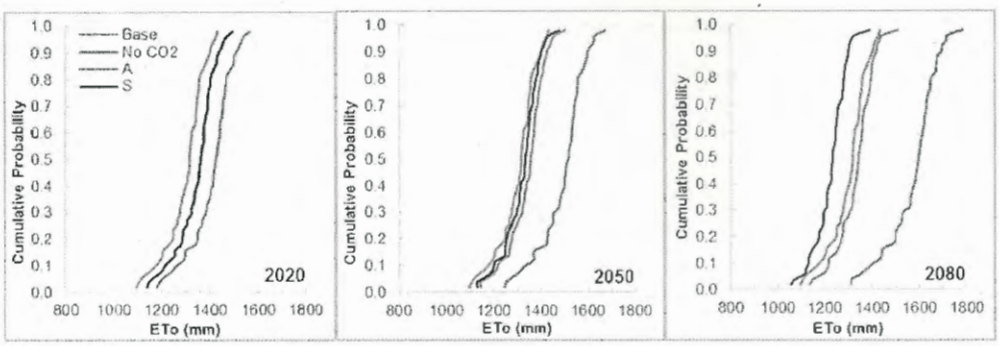

(a) Scenario S1: ensembles of 112 projections covering all three emission paths.

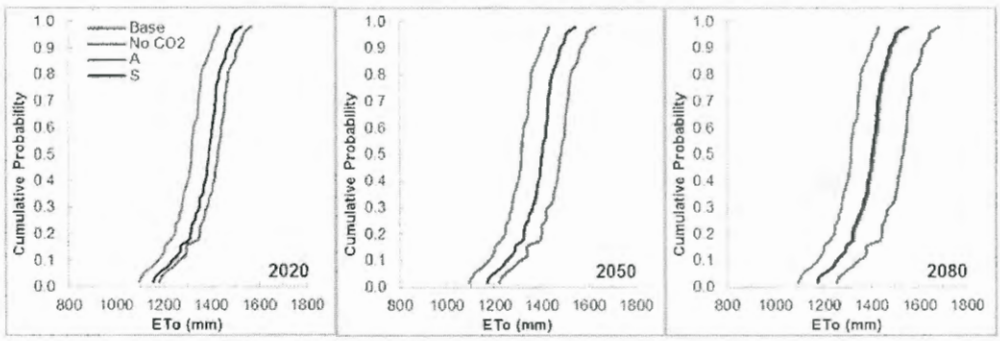

(b) Scenario S2: ensembles of 37 projections representing the B1 (low) emission scenario.

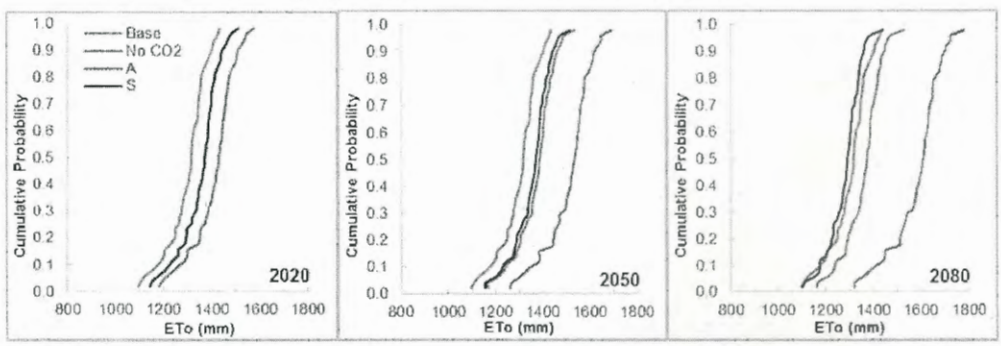

(c) Scenario S3: ensembles of 39 projections representing the A1B (medium) emission scenario.

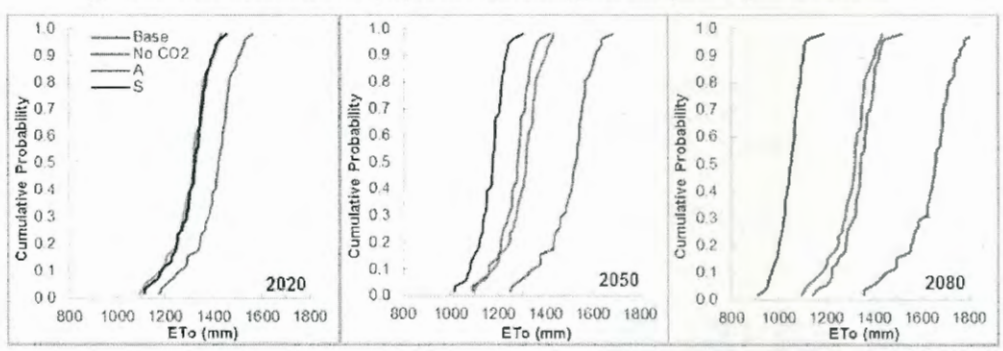

(d) Scenario S4: ensembles of 36 projections representing the A2 (high) emission scenario

Figure 4. Projected effect of climate changes on the probability distribution function of annual ET_o during the 2020s, 2050s, and 2080s, with and without considering the effect of CO_2 levels under different climate change scenarios. "No CO_2" indicates that the effect of CO_2 levels is not considered, "A" indicates CO_2 effects included using the Allen (1990) equation 5, and "S" indicates CO_2 effects included using the Stockle et al. (1992) equation 4.

Table 3. Projected changes in reference evapotranspiration with and without considering the effects of CO_2 levels under different projected climate change scenarios.

Scenario and Period[a]	CO_2 (ppm)[b]	Reference Evapotranspiration (mm d^{-1})												
		Jan.	Feb.	Mar.	Apr.	May	June	July	Aug.	Sept.	Oct.	Nov.	Dec.	Annual[c]
Base	330	1.5	2.0	2.7	3.8	4.8	5.9	6.0	5.3	4.2	3.1	1.9	1.4	1300.4
S1: Ensembles of 112 projections covering all the three emission paths														
2020s	330	1.7	2.2	3.0	4.1	5.2	6.3	6.4	5.7	4.6	3.4	2.1	1.6	1408.2
2050s	330	1.9	2.4	3.2	4.3	5.5	6.5	6.6	5.9	4.9	3.7	2.3	1.8	1492.0
2080s	330	2.1	2.6	3.4	4.5	5.8	6.8	6.8	6.1	5.1	3.9	2.5	2.0	1573.8
2020s	460 A	1.6	2.0	2.8	3.8	5.0	6.1	6.2	5.5	4.4	3.2	1.9	1.5	1346.5
2050s	623 A	1.6	2.0	2.7	3.8	5.0	6.1	6.2	5.6	4.5	3.2	1.9	1.5	1340.6
2080s	790 A	1.6	2.0	2.6	3.7	4.9	6.0	6.2	5.6	4.5	3.2	1.9	1.4	1330.8
2020s	460 S	1.6	2.0	2.8	3.8	5.0	6.1	6.2	5.5	4.4	3.2	1.9	1.5	1345.9
2050s	623 S	1.5	1.9	2.7	3.7	4.9	6.0	6.2	5.5	4.4	3.2	1.9	1.4	1319.0
2080s	790 S	1.3	1.7	2.3	3.3	4.5	5.6	5.9	5.3	4.2	2.9	1.7	1.3	1224.7
S2: Ensembles of 37 projections representing the B1 (low) emission scenario														
2020s	330	1.7	2.2	3.0	4.1	5.2	6.2	6.4	5.7	4.6	3.4	2.1	1.6	1409.0
2050s	330	1.9	2.3	3.1	4.2	5.4	6.4	6.5	5.8	4.8	3.6	2.2	1.7	1462.4
2080s	330	2.0	2.5	3.2	4.4	5.6	6.6	6.6	5.9	4.9	3.7	2.3	1.8	1508.0
2020s	410 A	1.7	2.1	2.9	4.0	5.1	6.1	6.3	5.6	4.5	3.3	2.0	1.6	1371.8
2050s	480 A	1.7	2.1	2.9	4.0	5.1	6.2	6.4	5.6	4.6	3.4	2.0	1.6	1388.6
2080s	550 A	1.7	2.2	2.9	4.0	5.2	6.2	6.4	5.7	4.6	3.4	2.1	1.6	1394.5
2020s	410 S	1.7	2.1	2.9	4.0	5.1	6.1	6.3	5.6	4.5	3.3	2.0	1.6	1372.3
2050s	480 S	1.7	2.1	2.9	4.0	5.1	6.2	6.3	5.6	4.6	3.3	2.0	1.6	1386.9
2080s	550 S	1.7	2.1	2.9	3.9	5.1	6.2	6.3	5.6	4.6	3.4	2.0	1.6	1386.4
S3: Ensembles of 39 projections representing the A1B (medium) emission scenario														
2020s	330	1.7	2.2	3.0	4.1	5.2	6.3	6.4	5.7	4.6	3.4	2.1	1.6	1411.9
2050s	330	2.0	2.4	3.2	4.4	5.6	6.6	6.7	6.0	4.9	3.7	2.3	1.8	1510.9
2080s	330	2.1	2.6	3.4	4.6	5.8	6.8	6.8	6.2	5.2	3.9	2.5	2.0	1582.9
2020s	450 A	1.6	2.0	2.8	3.9	5.0	6.1	6.3	5.5	4.5	3.3	2.0	1.5	1355.2
2050s	600 A	1.6	2.0	2.8	3.9	5.1	6.2	6.3	5.6	4.6	3.3	2.0	1.5	1370.5
2080s	750 A	1.6	2.0	2.7	3.8	5.0	6.1	6.3	5.6	4.6	3.3	2.0	1.5	1357.4
2020s	450 S	1.6	2.0	2.8	3.9	5.0	6.1	6.2	5.5	4.5	3.3	2.0	1.5	1354.8
2050s	600 S	1.6	2.0	2.7	3.8	5.0	6.1	6.3	5.6	4.5	3.3	1.9	1.5	1354.0
2080s	750 S	1.5	1.8	2.5	3.5	4.7	5.8	6.1	5.4	4.4	3.1	1.8	1.4	1279.9
S4: Ensembles of 36 projections representing the A2 (high) emission scenario														
2020s	330	1.7	2.2	3.0	4.0	5.2	6.2	6.4	5.6	4.6	3.4	2.1	1.6	1403.7
2050s	330	1.9	2.4	3.2	4.3	5.5	6.6	6.7	6.0	4.9	3.7	2.3	1.8	1502.1
2080s	330	2.2	2.7	3.5	4.7	6.0	7.0	7.0	6.3	5.3	4.1	2.6	2.1	1632.6
2020s	520 A	1.5	1.9	2.7	3.7	4.9	5.9	6.1	5.4	4.3	3.1	1.9	1.4	1311.9
2050s	790 A	1.4	1.8	2.5	3.5	4.7	5.8	6.1	5.4	4.3	3.0	1.8	1.3	1267.9
2080s	930 A	1.5	1.9	2.6	3.7	4.9	6.1	6.3	5.6	4.5	3.3	1.9	1.4	1335.6
2020s	520 S	1.5	1.9	2.7	3.7	4.8	5.9	6.1	5.4	4.3	3.1	1.9	1.4	1307.4
2050s	790 S	1.2	1.6	2.2	3.2	4.3	5.5	5.8	5.1	4.0	2.7	1.5	1.2	1165.9
2080s	930 S	1.0	1.3	1.8	2.7	3.8	5.0	5.4	4.8	3.7	2.4	1.3	1.0	1044.0

[a] Base = ET_o with respect to base value (no change in temperature and CO_2); 2020s = 2010-2039, 2050s = 2040-2069, and 2080s = 2070-2099.
[b] A = Allen (1990) equation 5 is used for CO_2 effects, and S = Stockle et al. (1992) equation 4 is used for CO_2 effects.
[c] Annual ET_o in mm.

To get an idea of changes in ET_o for taller crops, we also simulated ET_o with a tall crop (similar to alfalfa) reference surface [with numerator (C_n) and denominator (C_d) constants of 1600 °C mm s^3 Mg^{-1} s^{-1} and 0.38 s m^{-1}, as compared to C_n = 900 °C mm s^3 Mg^{-1} s^{-1} and C_d = 0.34 s m^{-1} in the FAO-56 PM equation (eq. 2) for a short crop similar to grass] for daily reference ET_o (ASCE-EWRI, 2005). The results showed that the annual ET_o estimated using the tall grass reference was about 1.35 times higher than short grass reference ET_o (fig. 5). When the effect of CO_2 on stomatal conductance was simulated within the PM equation using the C4 (maize) equation (Allen, 1990), it resulted in lower ET_o estimates as compared to that of ET_o estimated using the C3 (soybean) equation (fig. 5). For example, during 2080 under the S1 scenario (ensembles of all 112 projections), changes in the annual ET_o were about 2.4% and -2.8% for C3 (soybean) and C4 (maize) crops, respectively, when ET_o was estimated using a short crop (similar to grass) reference surface PM equation. In the case of a tall crop (similar to alfalfa), the changes ET_o were about 3.9% and -1.8% for C3 (soybean) and C4 (maize) crops, respectively, during the 2080s under the S1 scenario.

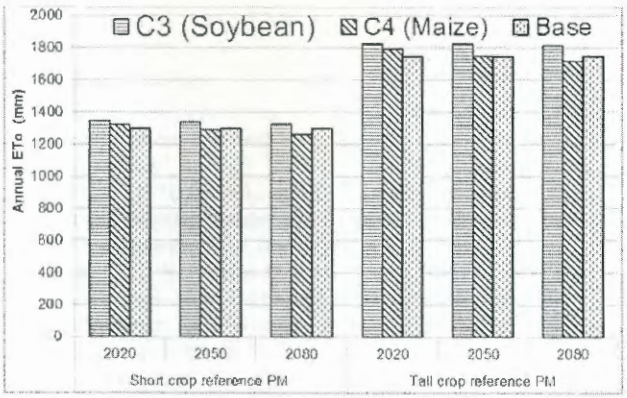

Figure 5. Annual ET_o for C3 and C4 crops estimated using the PM equation with short and tall crop reference surfaces.

Thus, changes in ET_o depend on the scenarios considered, month or season of the year, reference surface considered for the PM equation, and how the effect of changes in the stomatal resistance term (due to change in CO_2 levels) is included in the PM equation.

The results presented in this study indicate plausible changes in ET_o under projected changes in temperature and increased atmospheric CO_2 concentrations. The ET_o was estimated following the guidelines suggested for estimation of ET_o using the FAO-56 Penman-Monteith method. This method has been recommended as the sole standard method and has been applied in wide range of locations and climatic conditions. One of the major limitations of this method is its relatively high data requirement. This method is based on a hypothetical reference crop with an assumed crop height of 0.12 m and a fixed surface resistance of 70 s m^{-1}. The surface resistance varies with time of day and with time of year. Assuming a constant surface resistance term is perceived as weakness of this method, as surface resistance may change with climate and weather parameters, variation in day length, or differences between daytime and nighttime wind (Pereira et al., 1999). The effect of plant physiology is considered by a stomatal conductance term in the equation, which again varies from one crop to another, and different varieties can be affected differently. Gholipoora et al. (2010) reported marked variation among sorghum genotypes in transpiration response to VPD, with 17 genotypes identified as exhibiting a breakpoint in their VPD response in the range from 1.6 to 2.7 kPa, above which there was little or no further increase in transpiration. Paw U and Gao (1988) pointed out that the PM equation can introduce errors of up to 20% when the surface temperature exceeds the air temperature because the model uses a linearized form of the saturation vapor pressure function. However, they found that the PM equation yielded sufficiently accurate estimates of evapotranspiration when data from a semi-arid climate were used. McArthur (1990) reported that the value of the slope of the vapor pressure-temperature curve (Δ) depends on both surface and air temperature and suggested a simple iterative procedure to eliminate this error. In this study, the equations used for estimating the effect of increased CO_2 concentrations on stomatal conductance are assumed to remain valid for the stomatal conductance estimated using a 0.12 m tall C3 species of grass with a canopy resistance of 70 s m^{-1}. Most of the relationships describing plant physiological response to elevated CO_2 are based on controlled environment experiments (Allen, 1990; Long et al., 2006). However, there are large differences in reported changes in leaf area index and stomatal conductance among various experimental studies (Allen et al., 1991). Due to the uncertainty associated with projected climate change scenarios and uncertainties in the nature and magnitude of plant physiological response to climate change, there remains uncertainty in the precise magnitude of projected changes in ET_o. However, these simulation results provide valuable information on possible impacts of climate change on evapotranspiration demand, an important component of water balance and hydrological modeling studies.

Summary and Conclusions

For studying the effects of different projected climate change scenarios on reference evapotranspiration in future years (2020s, 2050s, and 2080s), four multi-model ensemble scenarios were generated from 112 bias-corrected and spatially disaggregated (BCSD) projections from the World Climate Research Program (WCRP) archive by varying the number of projections from 36 to 112. Results of the different simulation studies showed an increase in reference evapotranspiration (ET_o) with changing climate (increase in temperature, as projected by most GCMs), but the impact of increasing temperatures was almost offset by increasing CO_2 levels. Sensitivity analysis showed that the effect of a 1°C rise in temperature was offset by an increase in CO_2 levels up to 450 ppm, whereas the effect of a 2°C temperature rise was offset by CO_2 concentrations of 660 ppm. The simulation results also showed that different empirical relationships used for incorporating the effect of CO_2 levels on stomatal conductance in the Penman-Monteith equation resulted in comparable ET_o at lower CO_2 concentrations, but at higher CO_2 levels there was large variations in estimated ET_o. The ensemble scenario generated using all the available 112 projections resulted in an 8.3%, 14.7%, and 21.0% increase in annual ET_o demand during the 2020s, 2050s, and 2080s, respectively. When the effect of CO_2 levels was considered along with changes in temperature, the changes in evapotranspiration demand varied in the range of 0.5% to 5.5%, -10.3% to 6.8%, and -19.7% to 7.2% during the 2020s, 2050s, and 2080s, respectively, depending on the climate change scenario and the equation used for estimating the effect of CO_2 level on stomatal conductance. The simulation results showed a variation in changes in ET_o demand depending on the climate change scenario, month of the year, and how the effect of changes in stomatal resistance due to increasing CO_2 concentrations were considered.

Acknowledgements

The first author would like to thank the USDA Foreign Agricultural Service (FAS) for providing the necessary funding under the Global Research Alliance and the Norman E. Borlaug International Agricultural Science and Technology Fellowship Program for conducting this research work.

References

Allen, L. H. 1990. Plant response to rising carbon dioxide and potential interaction with air pollutants. *J. Environ. Qual.* 19(1): 15-34.

Allen, R. G., F. N. Gichuki, and C. Rosenzweig. 1991. CO_2-induced climatic changes and irrigation-water requirements. *J. Water Resources Plan. and Mgmt.* 117(2): 157-178.

Allen, R. G., L. S. Pereira, D. Raes, and M. Smith. 1998. Crop evapotranspiration: Guidelines for computing crop water requirements. FAO Irrigation and Drainage Paper 56. Rome, Italy: United Nations FAO.

ASCE-EWRI. 2005. The ASCE standardized reference evapotranspiration equation. R. G. Allen, I. A. Walter, R. L. Elliot, T. A. Howell, D. Itenfisu, M. E. Jensen, R. L. Snyder,

eds. Standardization of Reference Evapotranspiration Task Committee Final Report. Reston, Va.: ASCE Environmental and Water Resources Institute.

Christensen, N. S., and D. P. Lettenmaier. 2007. A multimodel ensemble approach to assessment of climate change impacts on the hydrology and water resources of the Colorado River basin. *Hydrol. Earth Syst. Sci.* 11(4): 1417-1434.

Easterling, W. E., N. J. Rosenberg, M. S. McKenney, C. A. Jones, P. T. Dyke, and J. R. Williams. 1992. Preparing the erosion productivity impact calculator (EPIC) model to simulate crop response to climate change and the direct effects of CO_2. *Agric. Forest Meteorol.* 59(1-2): 17-34.

Elgaali, E., L. A. Garcia, and D. S. Ojima. 2007. High-resolution modeling of the regional impacts of climate change on irrigation water demand. *Climatic Change* 84(3-4): 441-461.

Ficklin, D. L., Y. Luo, E. Luedeling, and M. Zhang. 2009. Climate change sensitivity assessment of a highly agricultural watershed using SWAT. *J. Hydrol.* 374(1-2): 16-29.

Field, C. B., R. B. Jackson, and H. A. Mooney. 1995. Stomatal responses to increased CO_2: Implications from the plant to the global scale. *Plant, Cell and Environ.* 18(10): 1214-1225.

Gholipoora, M., P. V. Vara Prasad, R. N. Mutavab, and T. R. Sinclair. 2010. Genetic variability of transpiration response to vapor pressure deficit among sorghum genotypes. *Field Crops Res.* 119(1): 85-90.

Hamlet, A. F., E. P. Salathe, and P. Carrasco. 2010. Statistical downscaling techniques for global climate model simulations of temperature and precipitation with application to water resources planning studies. Seattle, Wash.: University of Washington, Climate Impacts Group. Available at: www.hydro.washington.edu/2860/. Accessed 16 May 2011.

Hay, L. E., R. L. Wilby, and G. H. Leavesley. 2000. A comparison of delta change and downscaled GCM scenarios for three mountainous basins in the United States. *J. American Water Resources Assoc.* 36(2): 387-397.

Hubbard, K. G., R. Mahmood, and C. Carlson. 2003. Estimating daily dew point temperature for the northern Great Plains using maximum and minimum temperature. *Agron. J.* 95(2): 323-328.

IPCC. 2007. *Climate Change 2007: The Physical Science Basis.* Contribution of Working Group I to the 4th Assessment Report of the Intergovernmental Panel on Climate Change (IPCC). Cambridge, U.K.: Cambridge University Press.

Irmak, S., J. O. Payero, D. L. Martin, A. Irmak, and T. A. Howell. 2006. Sensitivity analyses and sensitivity coefficients of standardized daily ASCE Penman-Monteith equation. *J. Irrig. and Drainage Eng.* 132(6): 564-578.

Kay, A. L., and H. N. Davies. 2008. Calculating potential evaporation from climate model data: A source of uncertainty for hydrological change impacts. *J. Hydrol.* 358(3-4): 221-239.

Kimball, B. A. 2007. Global changes and water resources. In *Irrigation of Agricultural Crops*, 627-653. 2nd ed. R. J. Lascano and R. E. Sojka, eds. Agronomy Monograph No. 30. Madison, Wisc.: ASA, CSSA, SSSA.

Kimball, B. A., and C. J. Bernacchi. 2006. Evapotranspiration, canopy temperature, and plant water relations. In *Managed Ecosystems and CO_2: Case Studies, Processes, and Perspectives*, 311-324. J. Noesberger, S. P. Long, R. J. Norby, M. Stitt, G. R. Hendrey, and H. Blum, eds. Berlin, Germany: Springer-Verlag.

Kingston, D. G., M. C. Todd, R. G. Taylor, J. R. Thompson, and N. W. Arnell. 2009. Uncertainty in the estimation of potential evapotranspiration under climate change. *Geophysical Res. Letters* 36: L20403, doi: 10.1029/2009GL040267.

Long, S. P., E. A. Ainsworth, A. D. B. Leakey, J. Nosberger, and D. R. Ort. 2006. Food for thought: Lower-than-expected crop yield stimulation using rising CO_2 concentrations. *Science* 312(5782): 1918-1921.

Martin, P., N. J. Rosenberg, and M. S. McKenney. 1989. Sensitivity of evapotranspiration in a wheat field, a forest, and a grassland to changes in climate and direct effects of carbon dioxide. *Climatic Change* 14(2): 117-151.

Maurer, E. P., L. Brekke, T. Pruitt, and P. B. Duffy. 2007. Fine-resolution climate projections enhance regional climate change impact studies. *Eos, Trans. AGU* 88(47): 504.

McArthur, A. J. 1990. An accurate solution to the Penman equation. *Agric. Forest Meteorol.* 51(1): 87-92.

McKenney, M. S., and N. J. Rosenberg. 1993. Sensitivity of some potential evapotranspiration estimation methods to climate change. *Agric. Forest Meteorol.* 64(1-2): 81-110.

Meehl, G. A., C. Covey, T. Delworth, M. Latif, B. McAvaney, J. F. B. Mitchell, R. J. Stouffer, and K. E. Taylor. 2007. The WCRP CMIP3 multi-model dataset: A new era in climatic change research. *Bull. American Meteorol. Soc.* 88(9): 1383-1394.

Morgan, J. A., D. R. LeCain, E. Pendall, D. M. Blumenthal, B. A. Kimball, Y. Carrillo, D. G. Williams, J. Heisler-White, F. A. Dijkstra, and M. West. 2011. C4 grasses prosper as carbon dioxide eliminates desiccation in warmed semi-arid grassland. *Nature* 476: 202-206.

Morison, J. I. L., and R. M. Gifford. 1983. Stomatal sensitivity to carbon dioxide and humidity: A comparison of two C3 and two C4 species. *Plant Physiol.* 71(4): 789-796.

Nash, I., and P. Gleick. 1991. Sensitivity of streamflow in the Colorado basin to climate changes. *J. Hydrol.* 125(3-4): 119-146.

Parajuli, P. B. 2010. Assessing sensitivity of hydrological response to climate change from forested watershed in Mississippi. *Hydrol. Proc.* 24(26): 3785-3797.

Paw U, K. T., and W. Gao. 1988. Applications of solutions to non-linear energy budget equations. *Agric. Forest Meteorol.* 43(2): 121-145.

Pereira, L. S., A. Perrier, R. G. Allen, and I. Alves. 1999. Evapotranspiration: concepts and future trends. *J. Irrig. and Drainage Eng.* 125(2): 45-51.

Raff, D. A., T. Pruitt, and L. D. Brekke. 2009. A framework for assessing flood frequency based on climate projection information. *Hydrol. Earth Syst. Sci.* 13(11): 2119-2136.

Ragab, R., and C. Prudhomme. 2002. Climate change and water resources management in arid and semi-arid regions: Prospective and challenges for the 21st century. *Biosystems Eng.* 81(1): 3-34.

Ramirez, J. A., and B. Finnerty. 1996. CO_2 and temperature effects on evapotranspiration and irrigated agriculture. *J. Irrig. and Drainage Eng.* 122(3): 155-163.

Ray, A. J., J. J. Barsugli, K. B. Averyt, K. Wolter, M. Hoerling, N. Doesken, B. Udal, and R. S. Webb. 2008. Climate change in Colorado: A synthesis to support water resources management and adaptation. Boulder, Colo.: University of Colorado, Western Water Assessment. Available at: http://cwcb.state.co.us/public-information/publications/Documents/ReportsStudies/ClimateChangeReportFull.pdf. Accessed 20 June 2001.

Reifen, C., and R. Toumi. 2009. Climate projections: Past performance no guarantee of future skill? *Geophysical Res. Letters* 36: L13704, doi: 10.1029/2009GL038082.

Rosenberg, N. J., M. S. McKenney, and P. Martin. 1989. Evapotranspiration in a greenhouse-warmed world: A review and a simulation. *Agric. Forest Meteorol.* 47(2-4): 303-320.

Saxe, H., D. S. Ellsworth, and J. Heath. 1998. Tree and forest functioning in an enriched CO_2 atmosphere. *New Phytol.* 139(3): 395-436.

Stockle, C. O., J. R. Williams, N. J. Rosenberg, and C. A. Jones. 1992. A method for estimating the direct and climatic effects

of rising atmospheric carbon dioxide on growth and yield of crops: Part 1. Modification of the EPIC model for climate change analysis. *Agric. Syst.* 38(3): 225-238.

Wand, S. J. E., G. F. Midgley, M. H. Jones, and P. S. Curtis. 1999. Responses of wild C4 and C3 grass (*Poaceae*) species to elevated atmospheric CO_2 concentration: A meta-analytic test of current theories and perceptions. *Global Change Biol.* 5(6): 723-741.

Wood, A. W., E. P. Maurer, A. Kumar, and D. P. Lettenmaier. 2002. Long-range experimental hydrologic forecasting for the eastern U.S. *J. Geophysical Res.* 107: 4429, doi:10.1029/2001JD000659.

Wu, Y., S. Liu, and. O. I. Abdul-Aziz. 2011. Hydrological effects of the increased CO_2 and climate change in the upper Mississippi River basin using a modified SWAT. *Climatic Change* 110(3-4): 977-1003.

Wullschleger, S. D., C. A. Gunderson, P. J. Hanson, K. B. Wilson, and R. J. Norby. 2002. Sensitivity of stomatal and canopy conductance to elevated CO_2 concentration: Interacting variables and perspectives of scale. *New Phytol.* 153(3): 485-496.